



5-2009

Local Head Loss of Non-Coaxial Emitters Inserted in Polyethylene Pipe

Oswaldo Rettore Neto
University of São Paulo, Brazil


Jarbas Honorio de Miranda
Universidade de São Paulo, Brazil

José Antonio Frizzzone
Universidade de São Paulo, Brazil

Stephen R. Workman
University of Kentucky, steve.workman@uky.edu

Right click to open a feedback form in a new tab to let us know how this document benefits you.

Follow this and additional works at: https://uknowledge.uky.edu/bae_facpub

 Part of the [Agricultural Science Commons](#), and the [Bioresource and Agricultural Engineering Commons](#)

Repository Citation

Neto, Oswaldo Rettore; de Miranda, Jarbas Honorio; Frizzzone, José Antonio; and Workman, Stephen R., "Local Head Loss of Non-Coaxial Emitters Inserted in Polyethylene Pipe" (2009). *Biosystems and Agricultural Engineering Faculty Publications*. 205.
https://uknowledge.uky.edu/bae_facpub/205

This Article is brought to you for free and open access by the Biosystems and Agricultural Engineering at UKnowledge. It has been accepted for inclusion in Biosystems and Agricultural Engineering Faculty Publications by an authorized administrator of UKnowledge. For more information, please contact UKnowledge@lsv.uky.edu.

Local Head Loss of Non-Coaxial Emitters Inserted in Polyethylene Pipe

Notes/Citation Information

Published in *Transactions of the ASABE*, v. 52, issue 3, p. 729-738.

© 2009 American Society of Agricultural and Biological Engineers

The copyright holder has granted the permission for posting the article here.

Digital Object Identifier (DOI)

<https://doi.org/10.13031/2013.27394>

LOCAL HEAD LOSS OF NON-COAXIAL EMITTERS INSERTED IN POLYETHYLENE PIPE

O. Rettore Neto, J. H. de Miranda, J. A. Frizzone, S. R. Workman

ABSTRACT. *The design of a lateral line for drip irrigation requires accurate evaluation of head losses in not only the pipe but in the emitters as well. A procedure was developed to determine localized head losses within the emitters by the formulation of a mathematical model that accounts for the obstruction caused by the insertion point. These localized losses can be significant when compared with the total head losses within the system due to the large number of emitters typically installed along the lateral line. An experiment was carried out by altering flow characteristics to create Reynolds numbers (R) from 7,480 to 32,597 to provide turbulent flow and a maximum velocity of 2.0 m s^{-1} . The geometry of the emitter was determined by an optical projector and sensor. An equation was formulated to facilitate the localized head loss calculation using the geometric characteristics of the emitter (emitter length, obstruction ratio, and contraction coefficient). The mathematical model was tested using laboratory measurements on four emitters. The local head loss was accurately estimated for the Uniram (difference of +13.6%) and Drip Net (difference of +7.7%) emitters, while appreciable deviations were found for the Twin Plus (-21.8%) and Tiran (+50%) emitters. The head loss estimated by the model was sensitive to the variations in the obstruction area of the emitter. However, the variations in the local head loss did not result in significant variations in the maximum length of the lateral lines. In general, for all the analyzed emitters, a 50% increase in the local head loss for the emitters resulted in less than an 8% reduction in the maximum lateral length.*

Keywords. *Contraction coefficient, Emitter, Head loss, Hydraulic radius.*

Drip irrigation pipes with integrated emitters alter the velocity of water at the location of the emitter insertion point, providing a significant localized head loss in addition to the head loss of the pipe, as demonstrated by Juana et al. (2002a). To obtain high uniformity of water distribution in operational units, the hydraulic system design should consider the total head loss in the pipe and the small variations in head loss of the emitters along the lateral line. However, the localized head losses are typically neglected because few equations exist for easily calculating these losses.

Since the head loss within the section of the emitter passage does not depend on the viscous forces (Bagarello et al., 1997; Juana et al., 2002b), a model to calculate the localized head loss contains variables that define the geometric relationships of the obstructing element and the

pipe. The main objective of this work was to formulate a mathematical model to estimate the localized head loss starting from an obstruction index of the emitter insertion point with applications of the conservation of energy and mass equations. Specifically, the obstruction affects the hydraulics of water inflow due to the abrupt reduction in cross-section of the pipe at the emitter and the subsequent return to full cross-section after the emitter.

THEORY

The emitter insertion point along the lateral line modifies the course of the water flow, causing local turbulence that results in localized head losses in addition to the losses distributed in the pipe. The turbulence is a consequence of the presence of the insertion point along the internal wall of the pipe, which causes an obstruction in the inflow section, a contraction in the insert place, and a reduction in the inflow pipe diameter (Al-Amoud, 1995; Bagarello et al., 1997; Juana et al., 2002a, 2002b; Provenzano and Pumo, 2004; Provenzano et al., 2005; Palau-Salvador et al., 2006).

For mathematical simplicity, many designers of irrigation projects prefer to use empirical equations like Hazen-Williams, Manning, and Scobey to determine the head losses instead of using the theoretical equation of Darcy-Weisbach. However, an important limitation of those empirical equations is a roughness factor assumed constant for all diameters and inflow speeds (Kamand, 1988). Due to that simplification, the head loss calculated by the empirical equations can differ significantly from the calculations by the Darcy-Weisbach equation in that the attrition factor varies with the inflow conditions (Bombardelli and García, 2003).

Submitted for review in January 2008 as manuscript number SW 7336; approved for publication by the Soil & Water Division of ASABE in April 2009.

The authors are **Oswaldo Rettore Neto**, Agricultural Engineer, Graduate Student, Department of Agricultural Engineering, Luiz de Queiroz College of Agriculture, University of São Paulo, Piracicaba, Brazil; **Jarbas Honorio Miranda**, Associate Professor, Department of Exact Sciences, Luiz de Queiroz College of Agriculture, University of São Paulo, Piracicaba, Brazil; **José Antonio Frizzone**, Full Professor, Department of Agricultural Engineering, Luiz de Queiroz College of Agriculture, University of São Paulo, Piracicaba, Brazil; and **Stephen R. Workman**, ASABE Member Engineer, Associate Professor, Department of Biosystems and Agricultural Engineering, University of Kentucky, Lexington, Kentucky. **Corresponding author:** Oswaldo Rettore Neto, Department of Agricultural Engineering, Luiz de Queiroz College of Agriculture, University of São Paulo, Av. Pádua Dias, 11 CP 9 CEP 13418-900, Piracicaba, SP, Brazil; phone: +55-19-3429-4217; fax: +55-19-3447-8571; e-mail: oretore@esalq.usp.br.

The energy dissipation represented by the head loss in turbulent inflow of real fluids through cylindrical tubes can be calculated by equations presented in the basic literature of hydraulics (Porto, 1998). The most important contribution is expressed by the equation of Darcy-Weisbach (Kamand, 1988; von Bernuth, 1990; Bagarello et al., 1995; Romeo et al., 2002; Sonnad and Goudar, 2006), whose form is expressed by (eq. 1):

$$hf = f \frac{L}{D} \frac{V^2}{2g} \quad (1)$$

where hf is head loss (m), L is pipe length (m), D is internal diameter (m), V is mean water velocity at uniform pipe sections (m s^{-1}), g is gravitational acceleration (m s^{-2}), and f is friction factor (dependent on the Reynolds number, R , and the roughness of the pipe wall, ϵ).

The hydraulic resistance, expressed as the friction factor (f), constitutes the basic information to the hydraulic project. From the pioneering contributions made by Weisbach in 1845, Darcy in 1857, Boussinesq in 1877, and Reynolds in 1895 mentioned in the work by Yoo and Singh (2005), the hydraulic resistance to flow has been the object of continual interest and study. Recently, the importance of head losses in drip irrigation has been recognized and has stimulated the development of mathematical equations to estimate them (Bagarello et al., 1997; Juana et al., 2002a, 2002b; Provenzano and Pumo, 2004; Provenzano et al., 2005; Palau-Salvador et al., 2006).

Previous experimental research (von Bernuth and Wilson, 1989; von Bernuth, 1990; Bagarello et al., 1995) showed that in small-diameter polyethylene pipes with Reynolds numbers (R) in the range $4,000 < R < 100,000$, the friction factor can be expressed by an equation similar to the Blasius equation (eq. 2):

$$f = c R^{m-2} \quad (2)$$

where c is a constant for the particular friction coefficient formula used, and m is the velocity (or flow rate) exponent.

Introducing $c = 0.316$ and $m = 1.75$ into the Blasius equation provides an accurate estimation of the frictional losses produced by turbulent flow inside uniform pipes with low wall roughness and Reynolds numbers within the range $4,000 < R < 100,000$ (Juana et al., 2002a, 2002b; Yildirim, 2006). According to the results of von Bernuth and Wilson (1989), c is a value in the range of 0.281 to 0.345. By using pipe head loss per unit length measurements obtained from 16, 20, and 25 mm nominal diameter pipes for R values ranging from 3,000 to 36,000, Bagarello et al. (1995) proposed two simple criteria of f estimation based, respectively, on a purely empirical approach and a semitheoretical analysis. According to the empirical approach, the c coefficient of the Blasius equation assumes a constant value equal to 0.302.

The local head loss (hf_e) in the emitters or around their connections with the lateral is due to the resistance caused by the transport of water around the obstructing element inside the pipe. This can be expressed in the classic form as a fraction of the kinetic load (K), obtained by the Reynolds similarity principle (eq. 3):

$$hf_e = K \frac{V^2}{2g} \quad (3)$$

where hf_e is local head loss (m), and K is coefficient of kinetic load.

The coefficient K depends on the geometric characteristics of the emitter insertion point and the Reynolds number (R). For a given pipe section (A), flow rate (Q), and for a connection with defined dimensions, the value of K is reduced with an increase of R until a limit is reached from which K remains approximately constant (Bagarello et al., 1997; Provenzano and Pumo, 2004). In practice, the effect of the viscous forces can be neglected for $R > 10,000$ according to Bagarello et al. (1997). In this case, the factor K can be expressed by geometric relationships considering the inflow section in the pipes and the obstructing element. For on-line emitters, the relationship between K and the geometry of the inflow section can be obtained using the theorem of B elanger, applied to a sudden contraction of the section and subsequent enlargement, in that section ($A_r = r \cdot A$), where r is the obstruction ratio, A_r represents the passage area for the fluid at the emitter insertion point, and A represents the passage area for the pipe without the emitter.

By applying the theorems of energy and mass conservation at a sudden enlargement among the sections A_c and A , we have the equation of B elanger (eq. 4):

$$hf_e = \frac{(V_c - V)^2}{2g} = \left(\frac{A}{A_r} - 1 \right)^2 \frac{V^2}{2g} \quad (4)$$

Equation 4 shows that the local loss due to a sudden enlargement depends on the ratio $IO = [(A - A_r)/A_r]^2$, named by Bagarello et al. (1997) as an obstruction index (eq. 5), which can be assumed representative of the obstruction due to both the emitter protrusion and the pipe deformation:

$$IO = \left(\frac{A}{A_r} - 1 \right)^2 = \left(\frac{1-r}{r} \right)^2 \quad (5)$$

where r is the obstruction ratio ($r = A_r/A$).

Similarly, the presence of an on-line emitter in a lateral determines a local loss (hf_e), due to the protrusion of emitter barbs into the flow, that can be expressed as a K fraction of the kinetic height. Previous experimental investigation carried out by Bagarello et al. (1997) showed that the K coefficient depends on the ratio between the pipe section (A) and the cross-section area (A_c) where the emitter is located, according to the following relationship:

$$K = 1.68 \left(\frac{A}{A_r} - 1 \right)^{1.29} \quad (6)$$

obtained in the range $1.00 < A/A_r < 1.40$.

Although each individual emitter usually determines a small local head loss given by equation 3, the sum of all such local losses in a lateral line can become significant, since emitter spacing can be very small and many emitters are inserted along a lateral line. Results of Al-Amoud (1995) indicate that there are significant energy losses due to the emitter connections. An increase in the energy loss of more than 32% compared to plain pipe was observed for laterals of 13 mm diameter.

The lateral lines of irrigation systems are made of flexible polyethylene of low density. Consequently, variations should

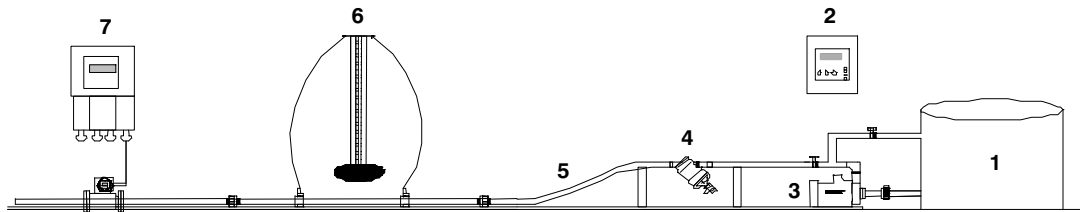


Figure 1. Layout of the experimental installation for lateral drip testing: 1 = water tank, 2 = variable frequency controller, 3 = pump, 4 = screen filter, 5 = drip lateral, 6 = differential manometer, and 7 = electromagnetic flowmeter.

be expected in the geometry along the pipe. These variations can hinder the determination of the necessary measurements relative to the obstruction index due to the emitter protrusion. The r values can be modified by the effect of the operation pressure on the internal pipe diameter depending on the polyethylene elasticity (Vilela et al., 2003). Therefore, the r estimate should be made with a statistical base using median values of A_r and A (Juana et al., 2002a).

MATERIALS AND METHODS

The research was carried out at the Irrigation Laboratory of the Department of Agricultural Engineering, University of São Paulo, Piracicaba, Brazil. A testing bench for head loss was built for the control, monitoring, and acquisition of the necessary data for the research development (fig. 1).

A variable frequency controller was connected to a pump to maintain a constant rotation of the pump to avoid flow alterations caused by any voltage variation in the electrical feed. It used water from the public network stored in a reservoir inside the laboratory and operated in closed circuit system. An in-line disk filter equivalent to 120-mesh screen was installed to remove particulates. Valves were connected to control the flow in the line entrance. A digital pressure monitor was used with range from 0 to 1,500 kPa and an accuracy of ± 1 kPa. During the tests, the pressure was maintained between 145 and 155 kPa to minimize the alteration of the pipe diameter, as described by Vilela et al. (2003).

The flow inside the pipe was measured by an inductive magnetic flowmeter ($\pm 1\%$ accuracy) installed at the end of the piping prior to the return to the reservoir. The head loss was measured by a differential manometer containing liquid with density 1.5 (times water density).

DEVELOPMENT OF THE CONNECTION FOR MEASUREMENT OF HEAD LOSS

A pipe segment 1 m in length was used for the head loss determination. Commercial barb connections could not be used in the test procedure because they would introduce additional head loss in the system, so a silicone hose (fig. 2) with a 10 mm external diameter and wall thickness of 2.5 mm was fitted to the pipe. The hose was cut in several segments of 25 mm length. The hose was fastened with a fast-drying glue, with the purpose of adhering the silicone segment to the pipe, so that the pipe center was in the center of the silicone hose segment.

MEASUREMENT OF THE FRICTION HEAD LOSS

A differential U-type manometer was used to measure head loss with a scale in mm (1,000 - 0 - 1,000). The



Figure 2. Silicone hose connection.

manometer was filled with a liquid having a density equal to 1.5 (times water density). The head loss was measured in a pipe segment 0.5 m in length. The manometer was connected to the test system using the silicone connection described above.

The experimental tests were accomplished by measuring the flow through the pipe and the pressure difference between two points as registered by the U-type manometer. The tests were conducted for 19 to 21 flow rates for each pipe and repeated for ten pipe samples. During the experiments, the water temperature was measured every 30 min using a mercury thermometer with a 0.1°C scale. It varied from 20.5°C to 24.5°C and was used to correct the kinematic viscosity of the water in the determination of head loss. An optic profile projector coupled to a microcomputer was used to determine the internal diameter of the pipe. Table 1 shows the diameter and wall thickness of the pipes used in the experiment.

The experimental values of the head loss were used to calculate f for equation 1, knowing the values of $V^2/2g$, L , and D . To determine the value of the c coefficient (eq. 7), a linear regression was performed between the values of f and $R^{-0.25}$.

$$f = \frac{c}{R^{-0.25}} \quad (7)$$

Table 1. Characteristics of pipes used in the experiment.^[a]

	Average (mm)	SD (mm)	CV (%)
Internal diameter	15.53	0.134	0.86
Wall thickness	1.07	0.06	5.61

[a] Ten samples were used to determine the characteristics.

Table 2. Characteristics of the emitters used in the experiment and the location of emitter within the pipe section.

Nominal diameter (mm)	Internal diameter (mm)	Manufacturer	Model	Flow (L h ⁻¹)	Emitter Spacing (m)	Connection Length (m)
17.5	15.53	Irrimon	Twin Plus	1.8	1.00	0.48
17	14.23	Netafim	Tiran	2.0	0.70	0.17
17	14.09	Netafim	Uniram	2.3	0.75	0.20
17	14.98	Netafim	Drip Net	1.6	0.75	0.20

To validate the methodology of using 0.5 m of pipe sections to determine the friction head loss, the friction factor, f , in the pipe was compared with that calculated by the model proposed by Bagarello et al. (1995). The experimental trials consisted of 193 measured pair points of flow head loss, in polyethylene pipe of 15.53 mm of internal diameter, resulting in Reynolds numbers ranging from 8,244 to 35,127.

DETERMINATION OF THE LOCAL HEAD LOSS DUE TO EMITTERS

Four types of emitters (Tiran, Uniram, Drip Net PC, and Twin Plus) were analyzed in the test apparatus and represented different geometric characteristics. Ten pipe samples were tested with each of the emitters. Due to the different spacing among emitters, three different lengths of pipe/emitter were used. These were 1.4 m for Tiran, 1.5 m for the Uniram and Drip Net PC, and 2.0 m for Twin Plus. After the initial tests, the emitters were sealed for subsequent tests so that the emitter obstruction could be evaluated. Table 2 contains the characteristics of the emitter/pipe combinations used in the experiment.

The head loss was determined between two points (1.0 m of pipe with emitter) for 15 flow values ranging from a low of 0.342 m³ h⁻¹ to a maximum of 1.201 m³ h⁻¹. The maximum flow corresponded to a maximum velocity of 2 m s⁻¹. The water temperature was measured with a thermometer for each test for subsequent use in the mathematical modeling.

For each discharge, the amount of local losses caused by the emitter was calculated by the difference between the total measured head losses of the 1.0 m segment with the sealed emitter and the corresponding friction losses evaluated by equations 1 and 2 for the section of pipe without an emitter, for $c = 0.296$. This procedure is in agreement with published research on local pressure losses for microirrigation laterals (Al-Amoud, 1995; Bagarello et al., 1997; Provenzano and Pumo, 2004).

DETERMINATION OF THE INFLOW SECTION

A key aspect of the experiment was the determination of the obstruction in the pipe created by the emitter. An optical projector (Starrett model HB 400) was used for this determination. The equipment projects a light beam on the object, which is enlarged by a magnifying glass. The image

is projected as a vertical image on a surface that contains the optical sensor. The platform holding the object being studied can move in vertical and horizontal directions to allow the entire object to be detected by the sensor. The optical projector was coupled to a personal computer with software developed by Metronics that interprets the signal sent by the sensor. With the integrated measurement system, it is possible to determine a point, straight line, diameter, distance, angle, and semicircles.

The determination of the cross-section of the emitter obstruction was accomplished in two stages. The first stage was the geometric characterization of the emitter obstruction with ten repetitions for each emitter/pipe combination. The second stage was the determination of the characteristics of the pipe. Table 3 shows the geometric characteristics of the emitters studied with the optical projector. Table 4 illustrates the shapes observed by the optical sensor for each of the emitters.

LOCAL HEAD LOSS MODEL

The head loss in pipes is inversely related to the pipe diameter. Since the water flow section along the emitter is not completely circular, the mathematical model for head loss in the emitter, hf_e , was calculated based on the hydraulic radius using the wetted perimeter (eq. 8):

$$R_h = \frac{A_r}{P_m} \quad (8)$$

where R_h is hydraulic radius, A_r is passage area of the fluid for the emitter, and P_m is wetted perimeter.

For the head loss determination in emitters, three components are considered: head loss in the entrance (hf_{en}), head loss in the emitter length (hf_{le}), and head loss in the exit (hf_{ex}). Figure 3 shows the representation of an emitter integrated to the lateral line with the respective considerations for the mathematical modeling.

Applying the Bernoulli theorem to sections 1 and 2 permits head loss determination in the entrance (hf_{en}):


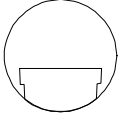
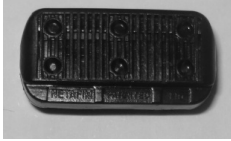
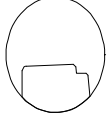
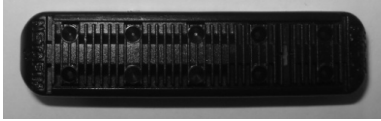
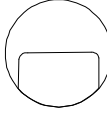

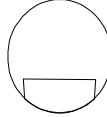
$$hf_{en} = \frac{V_c^2}{2g} - \frac{V_r^2}{2g} - \left(\frac{P_r}{\gamma} - \frac{P_c}{\gamma} \right) \quad (9)$$

Table 3. Geometric characteristics and inflow for the different emitters.

Emitter	Geometric Characteristics and Inflow ^[a]							
	Observed				Calculated			
	A mm ² (SD)	A_e mm ² (SD)	P_m mm (SD)	L_e mm (SD)	A_r mm ²	D_r mm	C_c mm	r mm
Twin plus	189 (3.27)	57.1 (0.561)	58.7 (0.241)	36.1 (0.111)	132	9.02	0.800	0.698
Tiran	159 (2.23)	35.9 (0.516)	49.1 (0.142)	72.0 (0.042)	123	10.0	0.816	0.774
Uniram	156 (1.48)	69.9 (2.28)	51.8 (0.553)	44.6 (0.153)	86.0	6.65	0.775	0.552
Drip net	176 (2.65)	53.7 (0.613)	52.8 (0.509)	21.5 (0.168)	122	9.28	0.796	0.695

^[a] Variables are defined in the Nomenclature section.

Table 4. Illustrations of the emitter geometry used.

Emitter	Top View	Frontal View
Twin Plus		
Drip Net		
Uniram		
Tiran		

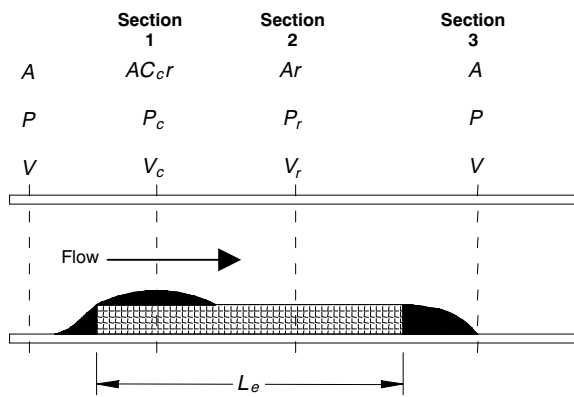


Figure 3. Diagram of typical longitudinal section of emitter line showing flow contraction and expansions.

where V_c is fluid velocity across the contracted section (m s^{-1}), V_r is fluid velocity through the emitter (m s^{-1}), γ is specific water weight (N m^{-3}), P_c is pressure in the pipe at the moment when the fluid passes through the entrance of the emitter (N m^{-2}), and P_r is pressure in the pipe when the fluid passes through the emitter (N m^{-2}).

Applying Newton's second law:

$$\begin{aligned}
 F &= m a \\
 &= \rho Q \Delta T a \\
 &= \rho Q \Delta T \frac{\Delta V}{\Delta T} \\
 &= \rho Q \Delta V \\
 &= \rho Q (V_c - V_r)
 \end{aligned} \quad (10)$$

where F is force (N), ρ is specific gravity (kg m^{-3}), Q is flow ($\text{m}^3 \text{s}^{-1}$), ΔT is time variation (s), a is acceleration (m s^{-2}), and ΔV is velocity variation (m s^{-1}).

By pressure definition, we can write:

$$F = (P_r - P_c) A_r \quad (11)$$

Comparing equations 10 and 11 and introducing the acceleration due to gravity yields:

$$\frac{(P_r - P_c)}{\gamma} = \frac{2V_r}{2g} (V_c - V_r) \quad (12)$$

Substituting equation 12 into equation 9 yields:

$$hf_{en} = \frac{(V_c - V_r)^2}{2g} \quad (13)$$

For $V_c = rC_c V$ and $V_r = V$, it becomes:

$$hf_{en} = \frac{V^2}{2g} \left(\frac{1}{rC_c} - 1 \right)^2 \quad (14)$$

Applying the Darcy-Weisbach equation, at the obstruction caused by the emitter (section 2 in fig. 3), with Blasius to determine head loss along the emitter length (hf_{le}) gives:

$$\begin{aligned}
 hf_{le} &= f \frac{L_e}{D_r} \frac{V_r^2}{2g} \\
 &= \frac{0.296}{R^{0.25}} \frac{L_e}{D_r} \frac{V_r^2}{2g} \\
 &= \frac{0.296}{2g} V_r^{1.75} \eta^{0.25} D_r^{-1.25} L_e
 \end{aligned} \quad (15)$$

where V_r is water velocity at the emitter section (m s^{-1}), D_r is diameter obtained from the hydraulic radius (m), L_e is emitter length (m), and η is kinematic water viscosity ($\text{m}^2 \text{s}^{-1}$). Diameter D_r is determined as:

$$D_r = 4R_h \quad (16)$$

where R_h is hydraulic radius (m).

Similarly to the entrance section, applying the Bernoulli theorem in the exit sections (sections 2 and 3) of the flow permits head loss determination in the exit (hf_{ex}):

$$\begin{aligned} hf_{ex} &= \frac{(V_r - V)^2}{2g} \\ &= \frac{(1-r)^2 V^2}{r^2 2g} \end{aligned} \quad (17)$$

Therefore, the equation for local head loss at the emitter can be expressed by the following equation:

$$\begin{aligned} hf_e &= \frac{V^2}{2g} \left(\frac{1}{C_c r} - \frac{1}{r} \right)^2 \\ &+ \frac{0.148}{g} V_r^{1.75} \eta^{0.25} D_r^{-1.25} L_e \\ &+ \left(\frac{1-r}{r} \right)^2 \frac{V^2}{2g} \end{aligned} \quad (18)$$

Equation 18 shows that the local losses are composed of three terms. The head loss at the entrance of the emitter, the head loss at the exit of the emitter, and the longitudinal head loss along the emitter.

For emitters integrated in the pipe, the contraction coefficient can be obtained by the approach developed by Juana et al. (2002 b), as (eq. 19):

$$\begin{aligned} C_c &= 0.907 - 0.523 (1-r) \\ &+ 0.659 (1-r)^2 - 0.321 (1-r)^3 \end{aligned} \quad (19)$$

RESULTS AND DISCUSSION

Figure 4 shows the curves for the friction factor, f , in the function for R previously fitted to the experimental data for the pipe with diameter 15.5 mm ($m = 1.75$). A c value of 0.296 was obtained for $7,480 < R < 32,597$ compared to values of 0.281 to 0.345 found by von Bernuth and Wilson (1989), 0.302 by Bagarello et al. (1995), and 0.300 by Cardoso et al. (2008) for low-density polyethylene pipe. The value found in this work confirms that the adopted procedure provides a good estimate of the friction factor for the studied pipe. A difference of 2% was found in relation to the value of c proposed by Bagarello et al. (1995) and a 6.3% difference to the original value of the Blasius equation. These differences can be justified as the increase in diameter of polyethylene pipe associated with increases in pressure (Vilela et al., 2003).

Figure 5 shows the relationships between the local head losses (hf_e) and the kinetic load ($V^2/2g$) for the studied emitters. The Tiran emitter presented the smallest coefficient of kinetic load ($K = 0.338$) and the Uniram emitter the largest coefficient ($K = 1.27$), corresponding, respectively, to the

smallest percentage of obstruction of the passage section (22.6%) and the largest (44.8%). The Drip Net emitter had the largest variation of the head loss values of the analyzed samples, caused by the larger differences of emitter insertion along the internal walls of the pipe.

The coefficient K depends on the Reynolds number and the geometric characteristics of the obstructing element. The values of K for each studied emitter varied slightly with R greater than 10,000 (fig. 6). For values of R less than 10,000, K increases with a reduction of R . This was also observed by Bagarello et al. (1997) and Provenzano and Pumo (2004). Therefore, the effect of the viscous force controls for $R > 10,000$ and K depends largely on the shape and size of the obstructing element so that an average value of K can be determined from the obstruction index.

The mathematical model was applied to each of the four tested emitters, and the estimated head loss was compared with the head loss measured in the laboratory (fig. 7). The Twin Plus emitter had a weaker correlation between the estimated and measured values of head loss (fig. 7a). On average, the model underestimated the head losses in the emitter by 55%. The local head loss estimated by the model for the Tiran emitter also deviated significantly from the measured head loss (fig. 7b). On average, the model overestimated the local head loss by 28.8%. This emitter presented the largest obstruction ratio (0.774) and the largest length (72.0 mm).

Figures 7c and 7d show a comparison of the calculated values of local head loss with the measured head loss for the Uniram and Drip Net emitters. These figures show the strong correlation between measured and estimated values, confirming that the model provided a good prediction of the head loss for those emitters.

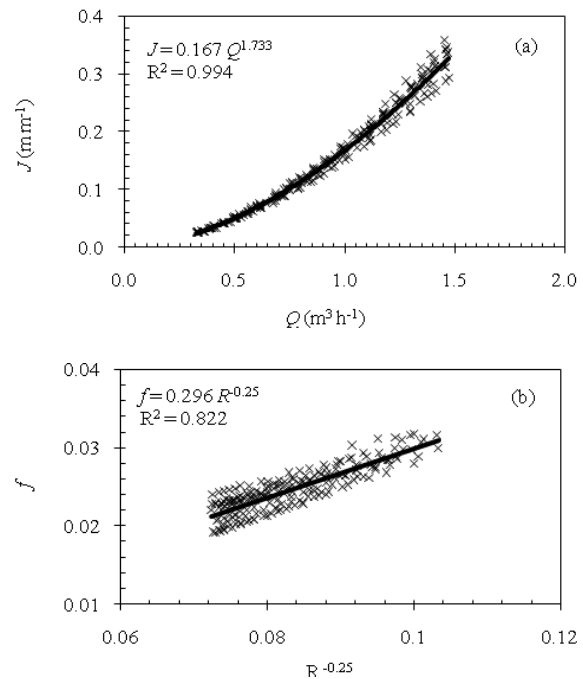


Figure 4. (a) Friction loss along the polyethylene pipe and (b) friction factor (f) and $R^{-0.25}$ relationship obtained by experimental data with $m = 0.25$.

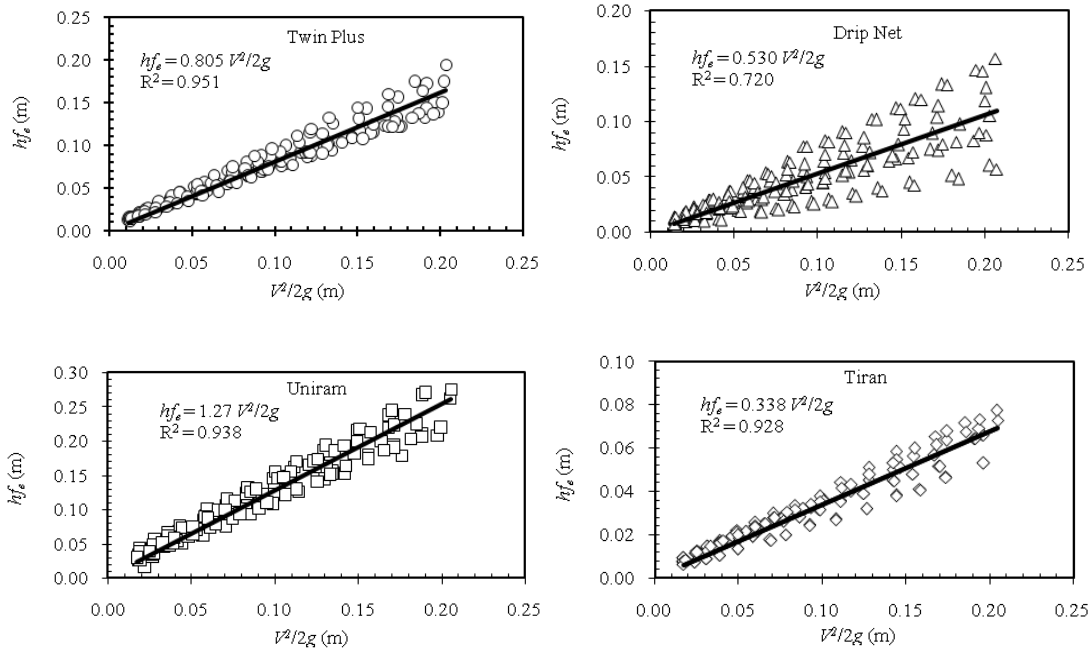


Figure 5. Local head loss at the emitter (h_{f_e} , m) in relation to kinetic load ($V^2/2g$, m).

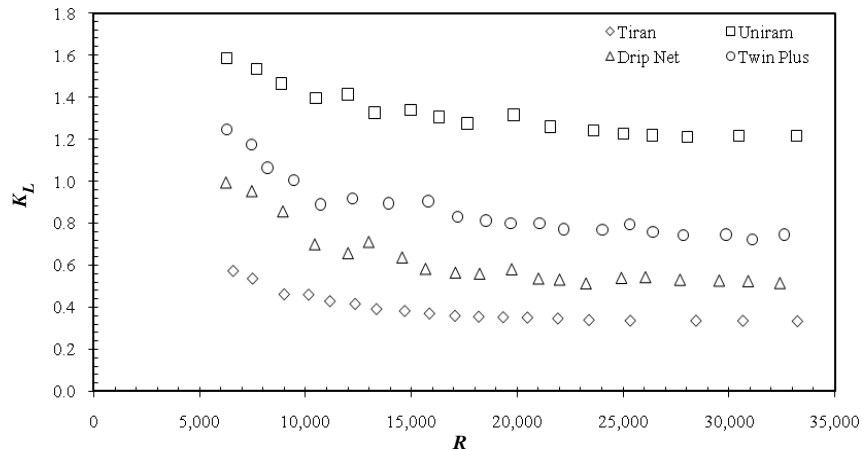


Figure 6. Observed average values of K in relation to R .

The accuracy in the h_{f_e} determination depends on the errors of the measurement of r and the C_c estimation. Consequently, the value of $C_c r$ will be affected. The Tiran emitter pipe is manufactured from a flexible material allowing an increase of internal diameter when pressurized, promoting an increase in r and reduction of h_{f_e} . This can be an important cause of lack of agreement of the model in relation to the observed values of h_{f_e} for integral drip tape. On the other hand, the Drip Net integral drip tape gave head losses comparable to the model, but the observed and predicted values showed a significant dispersion. This happened due to the poor alignment of the emitter with the axis of the pipe. The Uniram emitter, with better alignment with the pipe axis and larger rigidity of the pipe wall, gave the best comparison between the observed and estimated values. For the Twin Plus emitter, the experimental values of head loss were significantly larger than predicted, possibly as a result of the less hydrodynamic shape.

Simulations were used to estimate equivalent maximum lateral lengths for each of the drip lines. For each drip line

model, maximum lateral length was determined by two procedures: (I) the total amount of the local losses was calculated by a particular $h_{f_e}(V^2/2g)$ relationship for each emitter (fig. 5), and (II) the total amount of the local losses along the lateral was calculated by the proposed model (eq. 18). The maximum lateral lengths were determined using the step-by-step calculation, starting from the downstream end toward the upstream end of the drip line. Comparisons were made for the laterals placed on a zero slope and constant emitter flow rate for the emitters installed along the lateral, equal to 2.3, 1.6, and 1.8 $L h^{-1}$, respectively, for the Uniram, Drip Net, and Twin Plus emitters (table 5). These emitters were pressure compensating in the range of 100 to 350 kPa. The Tiran emitter was a non-compensating flow emitter with nominal flow rate equal to 2.0 $L h^{-1}$ and the following discharge-pressure head relationship: $q = 0.219 H^{0.48}$, where q is the emitter discharge ($L h^{-1}$) and H is the operating pressure (kPa).

For each compensating emitter model, the maximum pressure head at the upstream end of the lateral was assumed

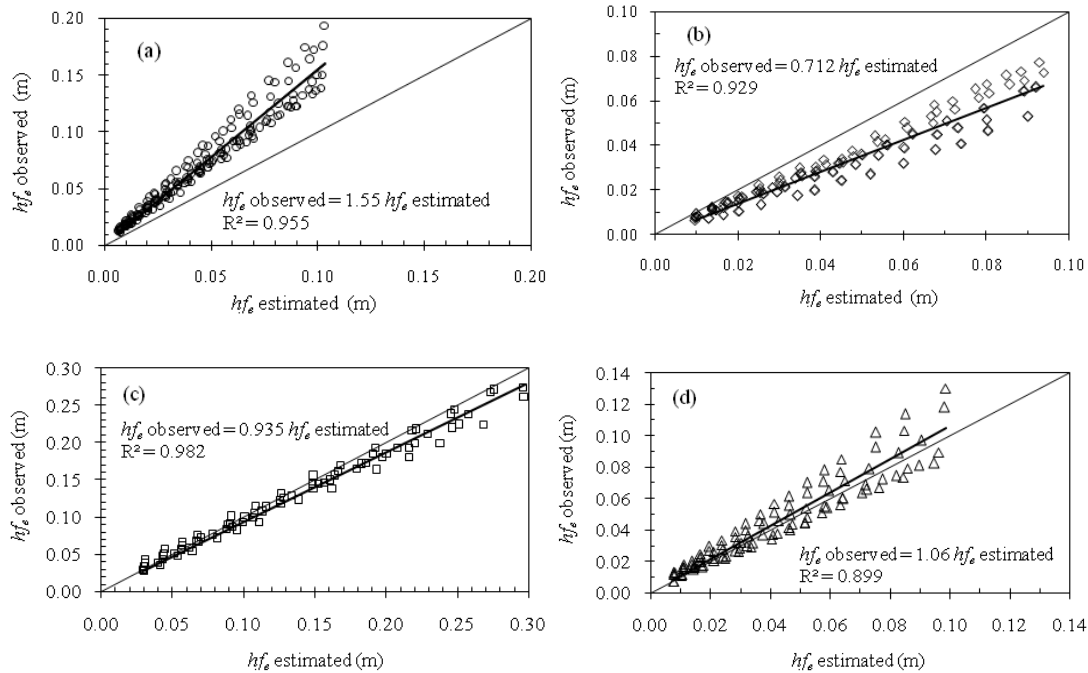


Figure 7. Comparison among the h_{f_e} estimated versus h_{f_e} observed for the (a) Twin Plus, (b) Tiran, (c) Uniram, and (d) Drip Net emitters.

Table 5. Comparison between maximum lateral length estimated with h_{f_e} calculated by a particular $h_{f_e}(V^2/2g)$ relationship for each emitter (procedure I) and by the proposed model (procedure II).

Parameter	Drip Line							
	Uniram		Drip Net		Twin Plus		Tiran	
	Procedure I	Procedure II	Procedure I	Procedure II	Procedure I	Procedure II	Procedure I	Procedure II
D (mm)	14.1	14.1	15.0	15.0	15.5	15.5	14.2	14.2
q_n (L h ⁻¹)	2.3	2.3	1.6	1.6	1.8	1.8	--	--
S_e (m)	0.75	0.75	0.75	0.75	1.0	1.0	0.70	0.70
L_e (mm)	--	44.6	--	21.5	--	36.1	--	72
D_r (mm)	--	6.57	--	9.28	--	9.02	--	9.98
C_c	--	0.775	--	0.796	--	0.800	--	0.816
Q_{in} (L h ⁻¹)	605	582	554	659	693	722	338	334
H_{in} (m)	24.9	25	24.9	25	25	25	12	12
H_{fin} (m)	10.0	10.0	10.0	10.0	10	10	9.6	9.6
H_{av} (m)	14.0	14.1	14.1	14.1	13.9	14	10.3	10.3
hf (m)	8.3	7.5	11.0	11.4	9.5	10.7	2.0	1.8
h_{f_e} (m)	6.6	7.5	3.9	3.6	5.5	4.3	0.4	0.6
hf_T (m)	14.9	15	14.9	15	15	15	2.4	2.4
Δh_{f_e} (%)	44.3	50.0	26.2	24.0	36.7	28.7	16.7	25.0
$h_{f_e var}$ (%)	--	+13.6	--	-7.7	--	-21.8	--	+50.0
L (m)	197.25	189.75	307.5	310.5	385	401	120.4	115.5
N	263	253	409	414	385	401	172	165
L_{var} (%)	--	-3.8	--	+1.0	--	+4.2	--	-4.1

to be 25 m and the minimum pressure head at the downstream end equal to 10 m. The Tiran emitter had a pressure variation equal to 20% along the lateral with the maximum pressure head at the inlet end equal to 12 m.

The hf for each segment S_e was calculated by equation 1, and substituting friction factor f by using $c = 0.296$ into the Blasius model for $4,000 \leq R \leq 10^5$, $f = 64/R$ for $R \leq 2,000$, and $f = 2.82 \times 10^{-7} R^{1.52}$ for $2,000 < R < 4,000$ (Silverberg and Manadili, 1997).

Simulations allowed separate evaluation of the friction losses along the uniform pipe (hf), local losses due to the emitters (h_{f_e}), total head losses along the lateral (hf_T), as well

as maximum lateral length (L) for a specified pressure variation (table 5).

Noticeable differences in total local losses ($h_{f_e var}$) were obtained for the Tiran (+50%) and Twin Plus (-21.8%) emitters. Although $h_{f_e var}$ differences were considerable, the effects on computed maximum lateral lengths (L) were of no practical significance. Procedure II underestimated L by 4.1% for the Tiran drip line and overestimated L by 4.2% for the Twin Plus drip line. For the Uniram and Drip Net lines, the proposed model provided better results for the local losses, with differences of +13.6% ($L_{var} = -3.8%$) and -7.7% ($L_{var} = 1%$), respectively.

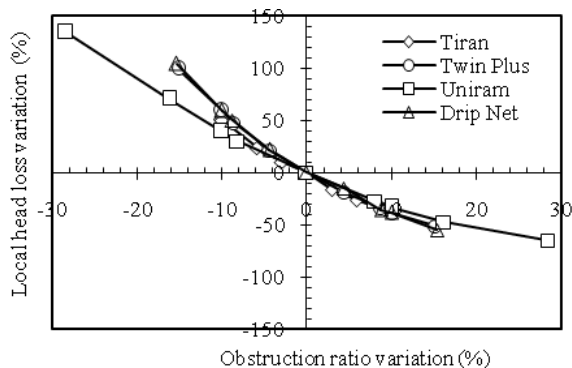


Figure 8. Local head loss variation as a function of the variation in obstruction ratio.

A sensitivity analysis of the model for calculating local head loss to the obstruction index was done by varying the emitter area between -35% to +35% (fig. 8). The maximum lateral line length for each emitter calculated by procedure II was taken as the reference for this analysis. The design criteria are shown in table 5, and the geometric characteristics of the emitters are presented in the table 3. The local head loss obtained by the model was sensitive to the variations in the obstruction ratio for all emitters. A reduction of 10% in the obstruction ratio for the Tiran emitter (increase of 34.3% in the emitter area) caused an increase of 50% in the local head loss. For the Twin Plus emitter, a reduction of 10% in the obstruction ratio (23% increase in the emitter area) caused an increase of 59% in local head loss.

The model underestimated the head loss by 55% from a 16% increase in the measure of the obstruction ratio (37% decrease in the emitter area) for the Twin Plus emitter (fig. 7a). Although the model for calculating head loss was sensitive to the variations in the obstruction ratio, the maximum length of the lateral lines was not affected as much (fig. 9). Although having a smaller obstruction ratio, the maximum length of the lateral line was greatest for the Uniram emitter. For the Twin Plus, Drip Net, and Tiran emitters, an increase of 50% in the local head loss caused small reductions of 5% in the maximum length of the lateral line. For the Uniram emitter, a 50% increase in the local head loss caused an 8% reduction in the maximum length of the lateral line. Reductions of local head loss by 50% caused small increases up to 10% in the length of the lateral lines.

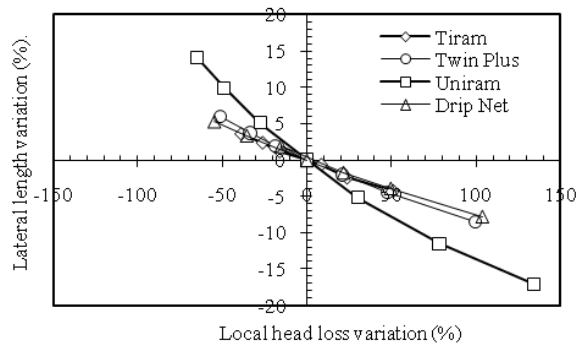


Figure 9. Variation of the maximum length of the lateral line as a function of the local head loss.

SUMMARY AND CONCLUSION

A model to estimate local head losses caused by a non-coaxial emitter integrated in a drip lateral line was derived based on principles of fluid mechanics and Bernoulli's theorem, thus allowing semi-empirical predictions. Local losses may thus be estimated *a priori*, and this can also be done when selecting emitters for microirrigation lateral line design.

To derive the local head loss, a model was considered as the sum of three components: the head loss due to the contraction of the cross-section area of the pipe, the head loss due to the insertion point, and the head losses within the emitter length calculated by the Darcy-Weisbach equation with the diameter calculated from hydraulic radius. The head losses at the contraction and the insertion point were dependent on the obstruction ratio, since the effects of viscous forces are negligible beyond a limiting Reynolds number value.

An experimental investigation was carried out to obtain the local losses for four integrated drip line emitters. The local losses were measured for each emitter in relation to the kinetic load, and K was obtained by linear regression analyses. The K value was assumed to be a characteristic of each emitter. The experimental local loss was compared to the model estimate. The local head loss was estimated with accuracy for the Uniram (difference of +13.6%) and Drip Net (difference of -7.7%) emitters, while appreciable deviations were found for the Twin Plus (-21.8%) and Tiran (+50%) emitters. The head loss estimated by the model was sensitive to the variations in the obstruction area of the emitter. However, the variations in the estimated local head loss did not result in significant variations in the maximum length of the lateral lines. In general, for all the analyzed emitters, a 50% increase in the local head loss resulted in less than an 8% reduction of the maximum length of the lateral, and a 50% decrease resulted in less than 10% increase in the length.

ACKNOWLEDGEMENTS

These authors are grateful to the following Brazilian Institutions for their financial support: Federal Department of Science and Technology (MCT), National Scientific and Technological Development Council (CNPq), São Paulo State Scientific Foundation (FAPESP), and National Institute of Science and Technology in Irrigation Engineering (INCTEI).

REFERENCES

- Al-Amoud, A. I. 1995. Significance of energy losses due to emitter connections in trickle irrigation lines. *J. Agric. Eng. Res.* 60(1): 1-5.
- Bagarello, V., V. Ferro, G. Provenzano, and D. Pumo. 1995. Experimental study on flow resistance law for small-diameter plastic pipes. *J. Irrig. Drain. Eng.* 121(5): 313-316.
- Bagarello, V., V. Ferro, G. Provenzano, and D. Pumo. 1997. Evaluating pressure losses in drip-irrigation lines. *J. Irrig. Drain. Eng.* 123(1): 1-7.
- Bombardelli, F. A., and H. Garcia. 2003. Hydraulic design of large-diameter pipes. *J. Hydraul. Eng.* 129(11): 839-846.
- Cardoso, G. G. G., J. A. Frizzone, and R. Rezende. 2008. Fator de atrito em tubos de polietileno de pequenos diâmetros. *Acta Sci. Agron.* 30(3): 299-305.

- Juana, L., L. Rodrigues-Sinobas, and A. Losada. 2002a. Determining minor head losses in drip irrigation laterals: I. Methodology. *J. Irrig. Drain. Eng.* 128(6): 376-384.
- Juana, L., L. Rodríguez-Sinobas, and A. Losada. 2002b. Determining minor head losses in drip irrigation laterals: II. Experimental study and validation. *J. Irrig. Drain. Eng.* 128(6): 385-396.
- Kamand, F. Z. 1988. Hydraulic friction factors for pipe flow. *J. Irrig. Drain. Eng.* 114(2): 311-323.
- Palau-Salvador, G., L. H. Sanchis, P. González-Altozano, and J. Arvizavalverde. 2006. Real local losses estimation for on-line emitters using empirical and numerical procedures. *J. Irrig. Drain. Eng.* 132(6): 522-530.
- Porto, R. M. 1998. *Hidráulica Básica*. São Carlos, Brazil: University of São Paulo, São Carlos School of Engineering.
- Provenzano, G., and D. Pumo. 2004. Experimental analysis of local pressure losses for microirrigation laterals. *J. Irrig. Drain. Eng.* 130(4): 318-324.
- Provenzano, G., D. Pumo, and P. Di Dio. 2005. Simplified procedure to evaluate head losses in drip irrigation lateral. *J. Irrig. Drain. Eng.* 131(6): 525-532.
- Romeo, E., C. Royo, and A. Monzón. 2002. Improved explicit equation for estimation of the friction factor in rough and smooth pipes. *Chem. Eng. J.* 86(3): 369-374.
- Silverberg, P. M., and G. Manadili. 1997. Replace implicit equations with signomial functions: A simple equation makes a user-friendly fit for friction chart. *Chem. Eng.* 104(1): 129.
- Sonnad, J. R., and C. T. Goudar. 2006. Turbulent flow friction factor calculation using a mathematically exact alternative to the Colebrook-White equation. *J. Hydraul. Eng.* 132(8): 863-867.
- Vilela, L. A. A., O. J. Soccol, E. S. Gervázio, J. A. Frizzone, and T. A. Botrel. 2003. Alteração no diâmetro de tubos de polietileno submetidos a diferentes pressões. *R. Brasileira Eng. Agríc. Ambiental.* 7(1): 182-185.
- von Bernuth, R. D. 1990. Simple and accurate friction loss equation for plastic pipe. *J. Irrig. Drain. Eng.* 116(2): 294-298.
- von Bernuth, R. D., and T. Wilson. 1989. Friction factors for small diameter plastic pipes. *J. Hydraul. Eng.* 115(2): 183-192.
- Yildirim, G. 2006. Hydraulic analysis and direct design of multiple outlets pipelines laid on flat and sloping lands. *J. Irrig. Drain. Eng.* 132(6): 537-552.
- Yoo, D. H., and V. P. Singh. 2005. Two methods for the computation of commercial pipe friction factors. *J. Hydraul. Eng.* 131(8): 694-704.
- A_e = emitter area (L^2)
- c = coefficient
- C_c = contraction coefficient
- D = internal diameter (L)
- D_r = diameter calculated from the hydraulic radius (L)
- F = force (F)
- f = friction factor of the Darcy-Weisbach equation
- g = acceleration due to gravity ($L T^{-2}$)
- H = operating pressure of the emitter ($F L^{-2}$)
- H_{av} = average pressure head ($F L^{-2}$)
- H_{in} = initial pressure head ($F L^{-2}$)
- H_{fin} = final pressure head ($F L^{-2}$)
- hf = friction losses along lateral (L)
- hf_e = local head loss (L)
- hf_T = total head loss along lateral (L)
- Δhf_e = amount of local loss expressed as a percentage of the total head loss
- $hf_{e\ var}$ = percent difference between local losses calculated by Procedure II and Procedure I
- IO = obstruction index
- K = coefficient of kinetic load
- L = pipe length (L)
- L_e = emitter length (L)
- L_{var} = lateral length variation
- m = exponent of the Blasius equation
- N = number of emitter instated in lateral
- P = pressure in the pipe after the emitter ($F L^{-2}$)
- P_c = pressure in the pipe at the moment when the fluid passes through the entrance of the emitter ($F L^{-2}$)
- P_m = wetted perimeter (L)
- P_r = pressure in the pipe when the fluid passes through the emitter ($F L^{-2}$)
- q_n = emitter nominal flow rate ($L^3 T^{-1}$)
- Q = flow ($L^3 T^{-1}$)
- Q_{in} = initial flow rate ($L^3 T^{-1}$)
- R = Reynolds number
- r = obstruction ratio
- R_h = hydraulic radius (L)
- S_e = emitter spacing (L)
- V = mean water velocity at uniform pipe sections ($L T^{-1}$)
- V_c = fluid velocity when passing by the emitter ($L T^{-1}$)
- V_r = fluid velocity through the emitter ($L T^{-1}$)
- γ = specific water weight ($F L^{-3}$)
- ρ = specific gravity of water ($F L^{-4} T^2$)
- η = kinematic viscosity of water ($L^{-2} T$)

NOMENCLATURE

- A = passage area of the fluid through the pipe without emitter (L^2)
- A_r = passage area of the fluid for the emitter (L^2)